

Travelling waves in a differential flow reactor with simple autocatalytic kinetics

J.H. MERKIN¹, R.A. SATNOIANU^{1,2} and S.K. SCOTT²

¹*Department of Applied Mathematical Studies, University of Leeds, Leeds, LS2 9JT, U.K.*

²*School of Chemistry, University of Leeds, Leeds, LS2 9JT, U.K.*

Received 30 January 1997; accepted in revised form 13 October 1997

Abstract. A simple prototype model for a differential flow reactor in which the possible initiation and propagation of a reaction-diffusion-convection travelling-wave solution (TWS) in the simple isothermal autocatalytic system $A + mB \rightarrow (m + 1)B$, rate kab^m ($m \geq 1$) is studied with special attention being paid to the most realistic cases ($m = 1, 2$). The physical problem considered is such that the reactant A (present initially at uniform concentration) is immobilised within the reactor. A reaction is then initiated by allowing the autocatalyst species to enter and to flow through the reaction region with a constant velocity. The structure of the permanent-form travelling waves supported by the system is considered and a solution obtained valid when the flow rate (of the autocatalyst) is very large. General properties of the corresponding initial-value problem (IVP) are derived and it is shown that the TWS are the only long-time solutions supported by the system. Finally, these results are complemented with numerical solutions of the IVP which confirm the analytical results and allow the influence of the parameters of the problem not accessible to the theoretical analysis to be determined.

Key words: waves, reaction-diffusion, autocatalytic, chemical instability.

1. Introduction

There is considerable current interest in the behaviour that can be supported by reaction-diffusion systems in which participating species have differing diffusivities, see for example [1–3]. The major impetus for such interest lies with the predictions of Alan Turing [4] who suggested that, for systems with appropriate kinetic feedback mechanisms, so-called ‘diffusion-driven’ instabilities may cause the spontaneous evolution to spatial patterns in initially homogeneous domains. The significance of such patterning for morphogenesis or animal coat markings have been explored [5] and recently Turing patterns have been created in the laboratory [6]. As discussed by Lengyel and Epstein [7], the practical requirements for this particular instability are not yet readily realised in available systems, primarily because of the current rudimentary state of selective control of individual species diffusivities. Recently, however, an alternative experimental device for producing a related effect has been proposed by Menzinger and Rovinsky [8–11], the ‘differential flow reactor’. This comprises a flow system in which one (or more) of the key species can be effectively immobilised with the remaining species flowing through the reactor producing an ‘open’ system. We can achieve this situation, for example, by creating the reaction domain as a matrix of ion exchange beads onto which selected species may become adsorbed via electrostatic interactions. Such a configuration has been employed by Menzinger and Rovinsky leading to a new kind of instability – the *differential-flow-induced chemical instability* (DIFICI). The requirements on the reaction kinetic mechanism underlying this phenomenon have been shown to be effectively equivalent to those underlying the Turing bifurcation but the conditions in terms of the diffusivities of feedback (activator) and reactant (inhibitor) species are different and perhaps more readily

accessible in practice. In the DIFICI case, the structures arising from the primary bifurcation in systems with ‘excitable’ kinetics comprise a train of travelling waves of permanent form propagating with constant velocity. The interaction of DIFICI and Turing instabilities has also been considered and shown to produce complex time dependent spatial structures including propagating stripes and spots [12].

In the present paper, we seek to investigate one of the fundamental ‘component processes’ leading to the DIFICI instability by pruning the kinetic mechanism to a single feedback process in the form of a single isolated autocatalytic step that, in a system without flow, would support a simple travelling wave front (with no subsequent recovery process). For an analysis of the DIFICI mechanism when applied to the cubic autocatalator kinetics in a finite reaction domain with periodic boundary conditions applied at its ends (as a model for a flow reactor with 100% recycling of the intermediate products) see [13].

We assume an isothermal system with kinetics of the form



where \bar{a}, \bar{b} are the concentrations of the reactant A and the autocatalyst B , k is the rate coefficient and m is the power of the autocatalytic step. We consider a situation in which only reactant A is present initially within the reactor at uniform concentration a_0 and that this species is immobilised within the reactor. We then initiated reaction by allowing the autocatalyst B to enter and to flow through the reaction region with a constant velocity u such that the flux which enters the reaction domain (from a reservoir in which B is in constant concentration) is proportional to the difference between the concentration at the inlet and the concentration in the reservoir (*i.e.* mathematically we will consider Robin boundary conditions). We make the further assumption (consistent with the experimental configuration) that the reactor is sufficiently long for end effects to be ignored and is sufficiently narrow so that transverse variations in concentrations can be neglected, with these then being described in terms of the co-ordinate \bar{x} measuring distance along the reactor.

This leads us to study the system of reaction-diffusion-advection equations:

$$\frac{\partial \bar{a}}{\partial \bar{t}} = -k\bar{a}\bar{b}^m, \quad (1.2)$$

$$\frac{\partial \bar{b}}{\partial \bar{t}} + u \frac{\partial \bar{b}}{\partial \bar{x}} = D_B \frac{\partial^2 \bar{b}}{\partial \bar{x}^2} + k\bar{a}\bar{b}^m, \quad (1.3)$$

on $\bar{t} > 0, 0 < \bar{x} < \infty$. The initial conditions are (from above)

$$\bar{a}(\bar{x}, 0) = a_0, \quad \bar{x} \geq 0, \quad \bar{b}(\bar{x}, 0) = 0, \quad \bar{x} > 0. \quad (1.4)$$

The boundary conditions for \bar{b} are of the Robin-type at $\bar{x} = 0$

$$D_B \frac{\partial \bar{b}}{\partial \bar{x}} = m_B(\bar{b} - \bar{b}_0), \quad \bar{t} \geq 0 \quad (1.5)$$

(where m_B is the mass-transfer coefficient and \bar{b}_0 is the reservoir concentration of B) and uniform conditions at large distance from origin

$$\bar{b} \rightarrow 0 \quad \text{as} \quad \bar{x} \rightarrow \infty, \quad \bar{t} \geq 0. \quad (1.6)$$

To make Equations (1.2–1.3) dimensionless we write

$$\bar{a} = a_0 a, \quad \bar{b} = a_0 b, \quad \bar{t} k a_0^m = t, \quad \bar{x} \left(\frac{k a_0^m}{D_B} \right)^{1/2} = x, \quad (1.7)$$

in terms of which Equations (1.2, 1.3) become

$$\frac{\partial a}{\partial t} = -ab^m, \quad (1.8)$$

$$\frac{\partial b}{\partial t} + \phi \frac{\partial b}{\partial x} = \frac{\partial^2 b}{\partial x^2} + ab^m, \quad (1.9)$$

with initial and boundary conditions

$$a(x, 0) = 1, \quad \text{on } x \geq 0, \quad b(x, 0) = 0, \quad \text{on } x > 0, \quad (1.10)$$

$$\frac{\partial b}{\partial x} = \mu(b - \beta_0) \quad \text{at } x = 0, \quad t \geq 0, \quad (1.11)$$

$$b \rightarrow 0 \quad \text{as } x \rightarrow \infty, \quad t \geq 0 \quad (1.12)$$

where the dimensionless parameters are

$$\phi = \frac{u}{(k a_0^m D_B)^{1/2}} \quad (\text{the flow parameter}), \quad \mu = \frac{m_B}{(k a_0^m D_B)^{1/2}}, \quad \beta_0 = \frac{b_0}{a_0}. \quad (1.13)$$

A system similar to (1.8–1.12) (but significantly without the flow term and with Dirichlet boundary conditions) has been considered by Metcalf *et al.* [14]. There the main interest was concerned with studying the possible initiation and structure of travelling wave solutions (TWS), especially when large powers of autocatalysis were taken. It was found that, for $m \geq 7.75$, the permanent form TWS that were supported by the system lost stability through longitudinal disturbances and an oscillatory wave structure was then obtained. For even higher values of m this oscillatory behaviour became unstable leading to a chaotic response.

In the present work we limit attention to much smaller but perhaps more realistic powers of autocatalysis, *i.e.* we consider the cases $m = 1, 2$, leading us to discuss the possible initiation and propagation of reaction-diffusion-advection waves in the above system with either quadratic or cubic autocatalysis. The main interest in using such an autocatalytic step is to consider the cases with $m = 1, 2$ which are the most physically relevant and have been successfully used to model real solution-phase kinetics (such as iodate-arsenous acid reaction [15], the Belousov–Zhabotinsky reaction [16]), radical chain-branching oxidation reactions [17], or enzyme reactions, such as glycolysis [18]. Reaction-diffusion waves in systems governed by such autocatalytic kinetics have been analysed previously in great detail (see [19–25]). However, we are concerned here with the change in behaviour of the long time solutions of our system caused by the changes in the flow parameter ϕ . We will pay attention also to the form of the boundary conditions which we impose at $x = 0$ (which are physically more realistic than Dirichlet boundary conditions as constant transfer between reservoir and the reactor is not possible to achieve in practice).

We start by considering the travelling waves of permanent form that are supported by Equations (1.8, 1.9).

2. Permanent-form travelling waves

Previous studies of systems described by autocatalytic kinetics, [14, 19–25] for example, have shown that a consideration of the corresponding travelling wave equations gives important insight into the nature of the full problem. We find this also to be the case here. A travelling wave solution (TWS) is a non-negative, nontrivial solution to Equations (1.8, 1.9) expressed in terms of the single travelling co-ordinate

$$y = x - vt, \quad (2.1)$$

where v is the constant wave speed.

Thus it is natural to study this class of solutions for the present model and we do so for the general situation when $m \geq 1$. This leads us to consider the travelling wave equations:

$$va' - ab^m = 0, \quad (2.2)$$

$$b'' + (v - \phi)b' + ab^m = 0 \quad (2.3)$$

on $-\infty < y < \infty$ (where primes denote differentiation with respect to y) subject to the boundary conditions

$$a \rightarrow 1, \quad b \rightarrow 0 \quad \text{as} \quad y \rightarrow \infty \quad (2.4)$$

(so that the wave is propagating into the unreacted part of the system) and that conditions are uniform at the rear of the wave. This requires that

$$a \rightarrow a_s, \quad b \rightarrow b_s \quad \text{as} \quad y \rightarrow -\infty, \quad (2.5)$$

where a_s and b_s are constant, which will depend on the parameters of the system and where, from the Equations (2.3, 2.4) at least one of a_s or b_s must be zero. Finally, we note that for a TWS to emerge as the long time solution of our initial-value problem (1.8–1.12) we must have that $v > 0$.

2.1. GENERAL PROPERTIES

The general properties of TWS (for the case where A is allowed to diffuse but without the flow term) have been given in Billingham and Needham [19] and Merkin *et al.* [23] and for the situation where A is immobile for general powers of m , again without flow, by Metcalf *et al.* [14]. There are, however, significant differences in the present situation so that we start by giving some general properties of TWS for our system.

P1: There are no TWS with $a \equiv 1$ or $b \equiv 0$. (This follows directly from Merkin *et al.* [23]).

P2: $a(y) > 0, b(y) > 0$ on $-\infty < y < \infty$ (follows directly from Merkin *et al.* [23]).

P3: $a_s = 0, v > \phi, b_s = \frac{v}{v-\phi} > 1$.

If we integrate Equation (2.3) once and apply boundary conditions (2.4, 2.5) we obtain

$$(v - \phi)b_s = \int_{-\infty}^{\infty} ab^m dy > 0, \quad (2.6)$$

from P2. Hence we must have $v > \phi$ and $b_s \neq 0$, from which it follows that $a_s = 0$, with the boundary conditions that must hold at the rear of the wave being

$$a \rightarrow 0, \quad b \rightarrow b_s > 0 \quad \text{as} \quad y \rightarrow -\infty. \quad (2.7)$$

If we now add Equations (2.2, 2.3), integrate once and apply boundary conditions (2.4) we obtain

$$b' + v(a + b - 1) - \phi b = 0. \quad (2.8)$$

Finally, if we now apply boundary conditions (2.7) we get

$$b_s = \frac{v}{v - \phi} > 1. \quad (2.9)$$

P4: a is strictly monotone increasing and $0 < a(y) < 1$.

This follows from (2.2, 2.4) and P3.

P5: b is strictly monotone decreasing and $b_s > b(y) > 0$ on $-\infty < y < \infty$.

Equation (2.3) can be written as

$$b' = -e^{(v-\phi)y} \int_{-\infty}^y e^{(v-\phi)s} a b^m ds < 0, \quad (2.10)$$

from P2 and the result follows.

$$\text{P6: } a + b > a + \frac{b}{b_s} > 1 \quad \text{on} \quad -\infty < y < \infty. \quad (2.11)$$

This results from Equation (2.8), P3 and P5 noting that (2.11) can be written as

$$1 - a - \left(\frac{v - \phi}{v} \right) b = \frac{b'}{v} < 0.$$

Finally, we obtain some bounds for the speed of propagation. To do so we combine Equations (2.2, 2.3, 2.8) in a single equation for b , namely

$$b'' + (v - \phi)b' + b^m \left(1 - \frac{b}{b_s} \right) - \frac{b'b^m}{v} = 0. \quad (2.12)$$

On integrating (2.12) we find that

$$\frac{b_s^{m+1}}{v(m+1)} - (v - \phi)b_s = - \int_{-\infty}^{\infty} b^{m+1} \left(1 - \frac{b}{b_s} \right) dy < 0, \quad (2.13)$$

(from P5) giving $(v - \phi)^2 > \frac{(b_s^{m-1}/m + 1)}{m + 1} > (1/m + 1)$ (from P3). Therefore

$$\text{P7: } v > \phi + (1/\sqrt{m + 1}).$$

The above bound does not appear to be very sharp as the following result shows, at least for the case $m = 1$ (quadratic autocatalysis).

$$\text{P8: In the case } m = 1, v \geq v_{\min} = \phi + 2.$$

To establish this result we require the behaviour of a TWS at the front of the wave. On linearizing Equation (2.3) around the steady-state (1,0) we find the asymptotic form

$$b'' + (v - \phi)b' + b = 0. \quad (2.14)$$

Equation (2.14) has solutions of the form $\exp(\lambda y)$ with $\lambda_{\pm} = \frac{1}{2}(\phi - v \pm \sqrt{(v - \phi)^2 - 4})$. We require the discriminant to be positive otherwise damped oscillatory solutions associated with

complex values of λ would result leading to negative (physically unacceptable) values for b . We also have that

$$v > v_{\min} \quad \text{then} \quad b \sim A_0 e^{\lambda-y} \quad \text{as} \quad y \rightarrow \infty, \quad (2.15)$$

$$v = v_{\min} \quad \text{then} \quad b \sim (A_0 y + B_0) e^{-y} \quad \text{as} \quad y \rightarrow \infty. \quad (2.16)$$

Finally, we note that, for $m = 1$ with $v = v_{\min}$

$$b_s = 1 + \frac{\phi}{2} \quad (2.17)$$

from P3.

2.2. SOLUTION FOR ϕ LARGE FOR CUBIC AUTOCATALYSIS

The wave speed for quadratic autocatalysis ($m = 1$) has already been given by P8. Here we develop an asymptotic solution for the system (2.2, 2.3) with $m = 2$ and subject to boundary conditions (2.4, 2.7) valid for $\phi \gg 1$. A consideration of the equations suggest that, for large ϕ , $v \sim \phi$ at leading order, which is also suggested by P8. This leads us to start our solution by putting

$$v = \phi + V\phi^{13}, \quad (2.18)$$

$$B = \phi^{-2/3}b, \quad (2.19)$$

$$Y = \phi^{1/3}y, \quad (2.20)$$

and leave a unscaled. This results in the equations

$$(1 + \phi^{-2/3}V)a' - aB^2 = 0, \quad (2.21)$$

$$B'' + VB' + aB^2 = 0, \quad (2.22)$$

subject to (from (2.4–2.7))

$$a \rightarrow 1, \quad B \rightarrow 0, \quad \text{as} \quad Y \rightarrow \infty, \quad (2.23)$$

$$a \rightarrow 0, \quad B \rightarrow B_s = \frac{1 + \phi^{-2/3}V}{V} \quad \text{as} \quad Y \rightarrow -\infty \quad (2.24)$$

(here primes denote differentiation with respect to Y). From (2.21–2.24) an expansion of the form

$$\begin{aligned} a(Y, \phi) &= a_0(Y) + \phi^{-2/3}a_1(Y) + \dots, \\ B(Y, \phi) &= B_0(Y) + \phi^{-2/3}B_1(Y) + \dots, \end{aligned} \quad (2.25)$$

$$V(\phi) = V_0 + \phi^{-2/3}V_1 + \dots$$

is suggested. At leading order we have

$$a_0' - a_0 B_0^2 = 0, \quad (2.26)$$

$$B_0'' + V_0 B_0' + a_0 B_0^2 = 0, \quad (2.27)$$

subject to (from (2.23–2.24))

$$a_0 \rightarrow 1, \quad B_0 \rightarrow 0 \quad \text{as } Y \rightarrow \infty, \quad (2.28)$$

$$a_0 \rightarrow 0, \quad B_0 \rightarrow \frac{1}{V_0} \quad \text{as } Y \rightarrow -\infty. \quad (2.29)$$

If we now add Equations (2.26, 2.27) and apply $\int_{-\infty}^{\infty} \cdots dY$ with boundary conditions (2.28, 2.29) we find that

$$B_0' = 1 - a_0 - V_0 B_0. \quad (2.30)$$

Thus we have to solve the Equations (2.26, 2.30) with boundary conditions (2.28, 2.29). A consideration of these equations along the general lines given in [20], shows that there is a unique minimum speed $V_{0,\min} > 0$ such that for all $V > V_{0,\min}$ the solution for B_0 has algebraic decay as $Y \rightarrow \infty$ and that the solution has exponential decay as $Y \rightarrow \infty$ only for $V_0 = V_{0,\min}$. To determine the solution and this minimum speed $V_0 = V_{0,\min}$ we have to proceed numerically, finding that

$$V_{0,\min} = 0.904977. \quad (2.31)$$

We are now in a position to compare these results, given by the asymptotic solution, with the full numerical solution of the initial system (2.2, 2.8). To do so note that, from (2.18, 2.19, 2.25)

$$v^{as} \sim \phi(1 + 0.904977\phi^{-2/3} + \cdots), \quad (2.32)$$

$$b_s^{as} \sim 1.105001\phi^{2/3} + \cdots \quad (2.33)$$

at leading order (where the superscript ‘*as*’ denotes asymptotic). In Figure 1a we show expression (2.32) by the dotted line, the agreement between the numerically computed values and those obtained from the asymptotic theory is extremely good even at quite moderate values of ϕ . This is not unexpected as a consideration of the higher order terms in the expansion leads to a leading order correction of $V_1\phi^{-2/3}$, with V_1 determined numerically as $V_1 = 0.28652$. As a further check of our asymptotic analysis we also plotted $(v - \phi)\phi^{-2/3}$ with v determined from the numerical solution of Equations (2.2, 2.8). The results are shown in Figure 1b, where they appear to be approaching the asymptotic value of $V_{0,\min}^{-1}$ as ϕ increases.

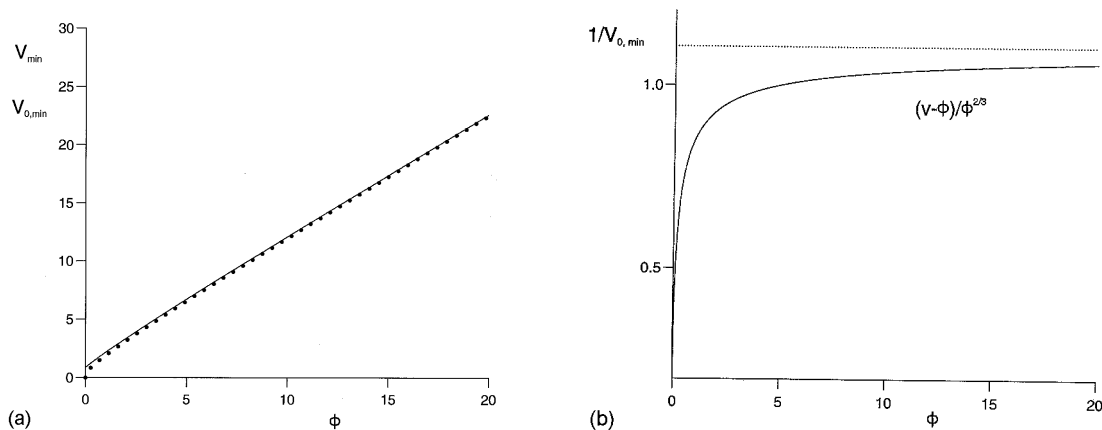


Figure 1. (a) A graph of the numerically computed minimum speed v_{\min} (plotted against ϕ) for the TWS for the case of cubic autocatalysis ($m = 2$). The dotted line represents the asymptotic expansion (2.32) and the full line the numerical speed obtained from an integration of the Equations (2.2, 2.8); (b) A graph of $(v - \phi)\phi^{-2/3}$ (against ϕ) with v as in Figure 1a (obtained from a numerical integration of Equations (2.2, 2.8)) showing the asymptotic approach to $V_{0,\min}^{-1}$. The numerical method used for these figures is similar to that explained in [14].

Finally we note that this analysis for $m = 2$ can be extended in an obvious way to general powers of m , for which the appropriate scalings are

$$v = \phi + \phi^\gamma V, \quad b = \phi^{2/(m+1)} B, \quad Y = \phi^\gamma y, \quad \gamma = \frac{m-1}{m+1} \quad (m > 1). \quad (2.34)$$

3. The initial-value problem

Here we consider the solution of the initial-value problem (IVP) (1.8–1.12) for the two cases $m = 1$ and $m = 2$. We start in 3.1 by proving that our IVP is well-posed (*i.e.* admits a unique solution at least locally in time). Then we show in 3.2 that the solution can be extended globally in time by giving a priori bounds for the solution in the cases $m = 1$ and $m = 2$. Finally, we discuss in 3.3 the numerical solutions of the IVP.

3.1. LOCAL EXISTENCE AND UNIQUENESS

Our main objective in this section is to show that the IVP (1.8–1.12) has local existence and uniqueness. The technical difficulty is having to work in an unbounded spatial domain.

R1: There is a $T_0 > 0$ such that the IVP (1.8–1.12) has a unique solution for $(x, t) \in (0, \infty) \times [0, T_0)$.

For the proof we apply the methods described in Henry [30]. To do so we need to recast our IVP in the following functional setting. We take $\Omega = (0, \infty)$ and

$$D(A) = C^2(\Omega) \times C^2(\Omega) \times R \quad (3.1)$$

and define the linear operator

$$A(u_1, u_2, \lambda) = \left(0, -\frac{d^2}{dx^2} + \phi \frac{d}{dx}, 0 \right), \quad (3.2)$$

provided $u_2 \rightarrow 0$ as $x \rightarrow \infty$ and $-(\partial u_2 / \partial x) + \mu u_2 = \lambda = \mu \beta_0$ on $x = 0$. We can then extend A to a linear closed operator in the usual way (which we will still denote by A) on $X = L^2(\Omega) \times L^2(\Omega) \times R$. A is then sectorial according to a result in Henry [30, pp. 20]. With

$$f: X_1 = D(A) \rightarrow X, \quad f(u_1, u_2, \lambda) = (-u_1 u_2^m, u_1 u_2^m, 0) \quad (3.3)$$

our IVP can be posed (with $U = (u_1, u_2, \lambda) \in X$) as

$$U_t + AU = f \quad \text{on } X, \quad U(0) = (1, 0, 0) \in X. \quad (3.4)$$

It is clear that $X_1 \subset L^2(\Omega) \times L^2(\Omega) \times R$ and that f is locally Lipschitz in U on X_1 . Thus we can apply Theorem 3.3.3 from Henry [30, pp. 54] and deduce that there is a $T_0 > 0$ such that the problem (3.4) has a unique solution on $(0, T_0)$. In fact we can readily show (using classical regularity theory results) that $U \in C^\infty(\Omega)$ for $0 < t < T_0$.

3.2. GLOBAL EXISTENCE AND UNIQUENESS

R2: Let $a(x, t), b(x, t)$ be a solution of our IVP for $(x, t) \in (0, \infty) \times [0, T]$, with $T > 0$ arbitrary. Then

$$0 \leq a(x, t) \leq 1, \quad 0 \leq b(x, t), \quad (3.5)$$

for all $(x, t) \in (0, \infty) \times [0, T]$.

(a) The proof for the left-hand inequality follows from the fact that the region $\Omega = \{(a, b), a, b \geq 0\}$ is a positively invariant region for IVP with initial conditions (1.10) in Ω for all $x > 0$. By considering the kinetic term $f = (-ab^m, ab^m)$ and taking due regard of the behaviour as $x \rightarrow \infty$ along the lines described by Merkin *et al.* [27] we see that the system (1.8, 1.9) is f -stable and the result follows by applying theorem 14.11 from Smoller [28].

(b) For the right-hand inequality for a we readily see that a is decreasing in t and from the initial condition (1.10) the result follows directly.

We now establish global existence, starting with the case $m = 1$ (quadratic autocatalysis). To do so we obtain a supersolution for b using scalar operators as follows. From (1.8) and R2 we readily deduce that

$$\frac{\partial b}{\partial t} - \frac{\partial^2 b}{\partial x^2} + \phi \frac{\partial b}{\partial x} - b = -b(1 - a) \leq 0, \quad (3.6)$$

for all $x, t > 0$. By considering the linear parabolic operator

$$L[u] = u_t - u_{xx} + \phi u_x - u, \quad (3.7)$$

we see that $\underline{u} = b$ and $\bar{u} = \beta_0 e^t$ are a subsolution and a supersolution respectively, since from (3.6), (1.9, 1.10, 1.11) we have that

$$L[\underline{u}] \leq 0 = L[\bar{u}], \quad \underline{u}(x, 0) = 0 \leq \beta_0 = \bar{u}(x, 0) \quad (3.8)$$

and at $x = 0, t > 0$

$$-\frac{\partial \underline{u}}{\partial x} + \mu \underline{u} = \mu \beta_0 \leq \mu \beta_0 e^t = -\frac{\partial \bar{u}}{\partial x} + \mu \bar{u}. \quad (3.9)$$

From (3.8, 3.9) it then follows, using the scalar comparison theorem for parabolic operators (Grindrod [29]), that for $m = 1$

$$\text{R3: } b(x, t) \leq \beta_0 e^t \quad \text{for all } x, t > 0. \quad (3.10)$$

Results R2 and R3, giving a priori bounds for the solutions of the IVP, then guarantee global existence and uniqueness (for $m = 1$), on applying Lemma 14.3 and Theorem 14.4 from Smoller [28].

A more refined analysis is required to obtain a similar result for b in the case $m = 2$ (cubic autocatalysis). To do this we apply an idea from Weissler [31] and start by consider the kinetic system associated to our IVP

$$a_t = -ab^2, \quad b_t = ab^2, \quad a(0) = 1, \quad b(0) = b_0 > 0. \quad (3.11)$$

It is readily deduced that solutions to (3.11) exist globally and are bounded for $t > 0$. In fact b is monotonically increasing with $b \rightarrow 1 + b_0$ as $t \rightarrow \infty$ and a is monotonically decreasing with $a \rightarrow 0$ as $t \rightarrow \infty$. We denote by $B(b_0, t)$ the solution to (3.11) for b .

Next we consider the following initial-value problem

$$u_t = u_{xx} - \phi u_x, \quad (3.12)$$

$$u(x, 0) = b_0, \quad -u_x + \mu u = \mu \beta_1 \quad \text{at } x = 0, \quad u \rightarrow \beta_2 \quad \text{as } x \rightarrow \infty, \quad (3.13)$$

with $\beta_1, \beta_2 > 0$. It is easily established that, for $\beta_1 \neq \beta_2$, (3.12–3.13) has a unique positive solution which we denote by $u(x, t)$, which is monotone on the spatial domain $(0, \infty)$. We now claim that, with appropriate choices for b_0, β_1, β_2 , $\bar{b}(x, t) = B(u(x, t), t)$ is an upper solution for b as a solution to our IVP (1.8–12). To see this note that

$$\bar{b}(x, 0) = b_0 > 0 = b(x, 0), \quad (3.14)$$

$$-\bar{b}_x + \mu \bar{b} = \mu \beta_1 \geq \mu \beta_0 = -b_x + \mu b \quad \text{at } x = 0, \quad t > 0 \quad \text{if } \beta_1 \geq \beta_0, \quad (3.15)$$

$$\bar{b} \rightarrow \beta_2 > 0 \quad \text{and } b \rightarrow 0 \quad \text{as } x \rightarrow \infty. \quad (3.16)$$

Also, for given x, t in our domain we consider the nonlinear parabolic operator

$$N[u] = u_t - u_{xx} + \phi u_x - au^2. \quad (3.17)$$

We note that (1.8) gives with initial conditions (1.10) that

$$a(x, t) = \exp\left(-\int_0^t b^m(x, s) ds\right) \leq 1 \quad (3.18)$$

and we have that a is a function of b only, thus giving N as a scalar operator. Then we have that

$$N[b] = 0, \quad (3.19)$$

$$N[\bar{b}] = B_u(u_t - u_{xx} + \phi u_x) + B_t - B_{uu}u_x^2 - (1 + u - B)B^2 = -B_{uu}u_x^2. \quad (3.20)$$

Thus we are naturally led to study the behaviour of $B(b_0, t)$ with respect with b_0 . We recall that from (3.11) we have $b_0 \leq B(b_0, t) < 1 + b_0$ for all $t \geq 0$. Furthermore, the following lemma gives the required information on the behaviour of the solution $B(b_0, t)$ with respect to the initial condition.

LEMMA 1. *For all $b_0 > 0$ we have*

- (1) $(\partial B / \partial b_0) > 0$ for all $t > 0$,
- (2) $(\partial^2 B / \partial b_0^2) \leq 0$ for all $t > 0$ and $b_0 > 0$ sufficiently large (in practice $b_0 > 25$ suffices).

The proof of these results is given in the Appendix. In view of result (2) of the above lemma we can always assure that the final term in (3.20) is positive. In fact we have from the above that

- (i) $B_u > 0$ for all $x, t > 0$,
- (ii) $B_{uu} \leq 0$ for all $x, t > 0$ and $u > 0$ sufficiently large.

To see that \bar{b} is an upper solution we notice that the solution u of the initial-value problem (3.13–3.14) can always be made sufficiently large with suitable choices for $b_0, \beta_1, \beta_2 > 0$, and we again conclude, on using the comparison theorem for the scalar parabolic operator N [29] that for $m = 2$

$$\text{R4. } b(x, t) \leq \bar{b}(x, t), \quad (3.21)$$

with \bar{b} uniformly bounded.

The a priori bounds given in R2 and R4 establish global existence and uniqueness for $m = 2$, again from Smoller [28]. An examination of these results (in particular the method of obtaining an upper solution for b when $m = 2$) shows that the method can be extended to general integer values of $m > 1$ in an obvious way, giving global existence and uniqueness for these cases as well. We expect from physical considerations (and this is also confirmed by the numerical results presented in the next section) that for each $m \geq 1$ the solutions to the corresponding IVP have global existence and uniqueness property. However, this is left unresolved at this stage.

Our results extend significantly the corresponding properties of the solutions to the IVP considered in previous work on simple autocatalytic reaction-diffusion systems (see [14] and references therein, for example) where upper bounds on the autocatalyst concentration were not given previously.

We now consider numerical solutions to the initial-value problem (1.8–1.12). These confirm our analytically derived predictions and extend the results to general values of the parameters.

3.3. NUMERICAL SOLUTIONS OF THE IVP

We solved the initial-value problem (1.8–1.12) using the method described in Merkin *et al.* [23]. This is essentially a Crank-Nicolson discretization method coupled with Newton-Raphson iteration to solve the systems of nonlinear algebraic equations that are formed at each time step. The algorithm allows an adjustable time step to be used so as to try and maintain a prescribed overall accuracy. We performed a relatively large set of numerical integrations by varying our parameters ϕ, μ, β_0 . In the results described below we chose representative values of these parameters (similar results were obtained for all the cases we tried).

We start our discussion by first taking the case with quadratic autocatalysis ($m = 1$). Figures 2a, 2b show concentration profiles for a and b , taken at equal time intervals for the case $\phi = 1.0$, $\mu = 1.0$, $\beta_0 = 1.0$. These profiles show the formation and propagation of travelling waves of permanent-form approaching a steady velocity as t increases. We have confirmed this by numerically computing the position and the velocity of the reaction-diffusion-advection fronts. This has been done by two different procedures (which enabled us to check the accuracy of each). Specifically we computed the position of the front as the point where $a(x, t) = 0.5$. Then these values were used to compute the velocity of the front by numerically differentiating (with central differences). The other procedure was to use an integral method which essentially used the approximated formula $x_w = \int_0^\infty (1 - a) dx$ (with x_w denoting the referenced front position and where the integral was computed using the trapezium method). Both these two methods gave very good agreement. We can see from Figure 2b that the travelling front left behind a region where $b = 1.5 = b_s$ (in agreement with the result P3). Also the large time velocity of the waves is, in this case, $v = 3 = v_{\min} = \phi + 2$ (the minimum speed as given from P8). This can be seen in Figure 4 where we plot the position of the travelling waves fronts evolved from the initial-value problem for the cases: $\phi = 0, 1, 5$ (with $\mu = 1.0$, $\beta_0 = 1.0$). We can see that in all the cases the front positions describe straight lines in time with constant slope giving the minimum speed $v_{\min} = \phi + 2$.

We have also studied the influence of the boundary condition at $x = 0$ by varying μ (the parameter related to the mass transfer of the autocatalyst). In Figure 3 we show the concentration profile of b for the case $\mu = 0.1$, $\phi = 1.0$, $\beta_0 = 1.0$ in order to compare it with the case in Figure 2b. Both graphs show that as time increases the concentration of the autocatalyst at the boundary $x = 0$ approaches that of the reservoir concentration β_0 or, equivalently,

$$\lim_{t \rightarrow \infty} \frac{\partial b}{\partial x} = 0, \quad (3.22)$$

(in which case the Robin boundary condition at $x = 0$ transforms to a Dirichlet type boundary condition) a result which shows that the long time structure arising from the initial-value problem is independent of the influence of the boundaries provided the flow reactor is very long. Also, our numerical integrations show (and the above figures depict) that the rate of this approach of b to β_0 at $x = 0$ is dependent on the value of μ , the larger the value of μ the faster the convergence. Another common feature seen in the b -profiles is that there is an initial over-production in the autocatalyst which is then spread out by convection and diffusion before the reaction becomes the dominant part. As expected this is less pronounced in the case in Figure 3 (smaller value of μ) comparing with that in Figure 2b. Finally, we add that result (3.22) was obtained in all the cases we tried.

Figures 5a, 5b show the influence of the reservoir concentration (reflected by β_0) upon the development of the travelling wave front. Here we took $\phi = 1.0$, $\mu = 1.0$ and we varied β_0 (by taking $\beta_0 = 2.0$ in Figures 5a and $\beta_0 = 0.5$ in Figure 5b). This corresponds to the opposing cases ‘over-driven’ and ‘under-driven’ in the autocatalyst concentration initiation, respectively. We see that in all the cases the long time wave structure which develops is independent of the value of β_0 leaving behind a region where $b = 1.5 = b_s$ and travelling with the minimum possible velocity $v = 3 = v_{\min} = \phi + 2$ as given by P3 and P8, respectively. In all cases the long time structure is a travelling reaction-diffusion wave of permanent form propagating with its minimum possible speed. At the rear of this is a region in which the

the concentration of reactant A is zero and that of autocatalyst B is b_s (as given by (2.7)). There is then an adjustment of this concentration to β_0 (the autocatalyst reservoir concentration) through a convection-diffusion wave which propagates with speed ϕ ($< v_{\min}$) and in which

$$b(x, t) \sim \beta_0 + \frac{(b_s - \beta_0)}{\sqrt{\pi}} \int_{-\infty}^{\eta} e^{-s^2} ds, \quad \eta = \frac{x - \phi t}{2\sqrt{t}}, \quad \text{as } t \rightarrow \infty. \quad (3.23)$$

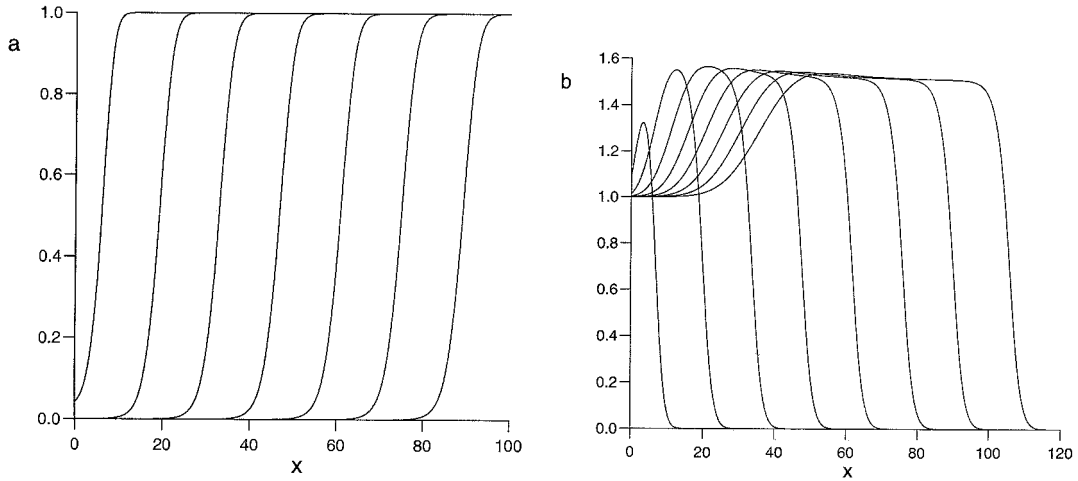


Figure 2. Concentration profiles shown at equal time intervals for $\phi = 1.0$, $\mu = 1.0$, $\beta_0 = 1.0$ for (a) a , (b) b (quadratic autocatalysis). We see the approach to a TWS travelling with constant velocity.

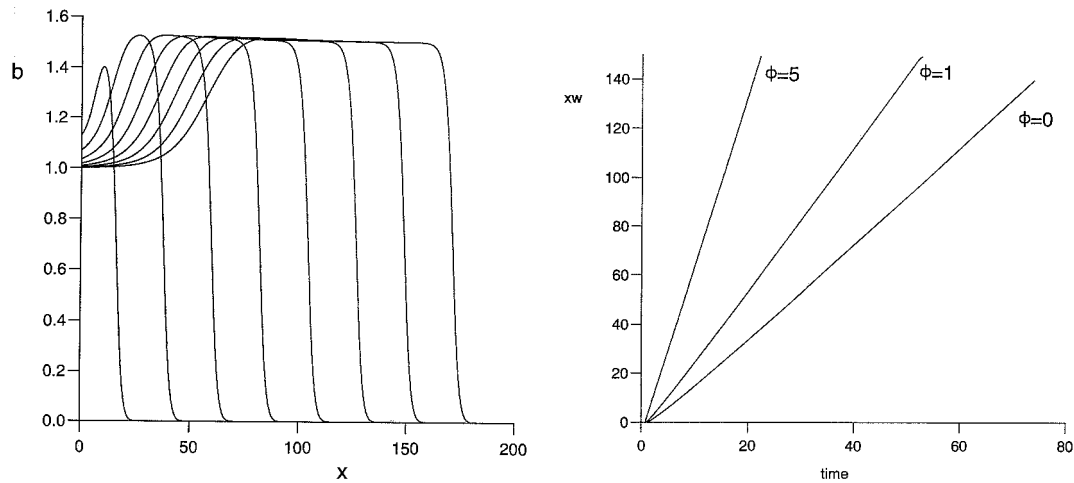


Figure 3. Concentration profile for b for $\phi = 1.0$, $\mu = 0.1$, $\beta_0 = 1.0$ (quadratic autocatalysis).

Figure 4. Successive positions of the TWS for the case $\mu = 1.0$, $\beta = 1.0$ and three different values of $\phi = 0, 1, 5$ (quadratic autocatalysis).

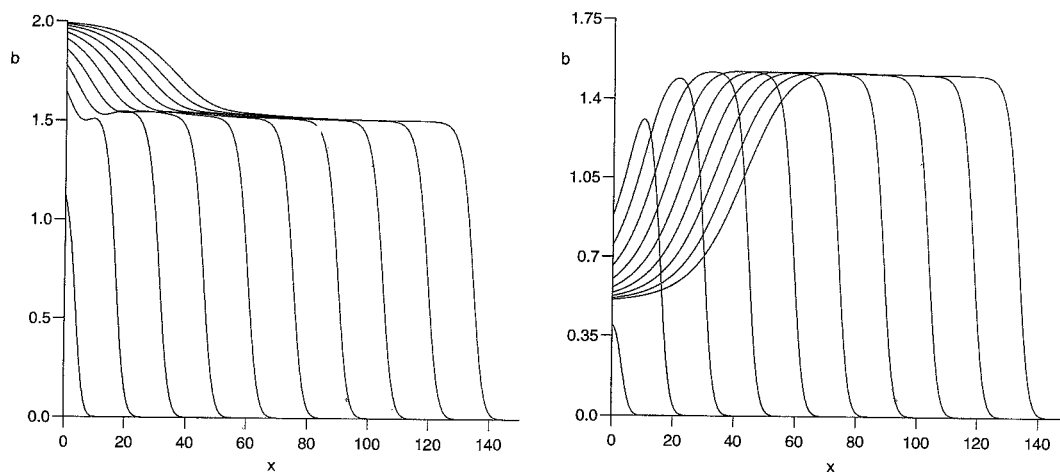


Figure 5. The influence of the boundary condition (quadratic autocatalysis): concentration profiles for b for $\phi = 1.0$, $\mu = 0.1$ and two different values of β_0 : (a) $\beta_0 = 0.5$, (b) $\beta_0 = 2.0$.

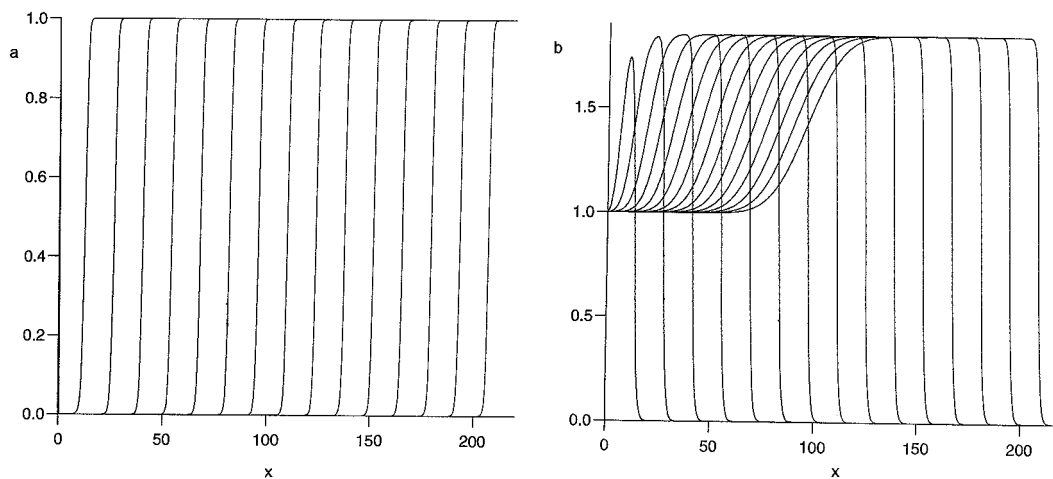


Figure 6. Concentration profiles for the case $\phi = 1.0$, $\beta_0 = 1.0$ for (a) a , (b) b (cubic autocatalysis).

We now consider the case of the cubic autocatalysis ($m = 2$). From the above discussion we have seen that any wave structure which develops as a long time solution of the initial-value problem (1.8–1.12) is in effect independent of the type of boundary condition applied at $x = 0$, provided this gives a correct qualitative description of the contact between the reservoir and the flow reactor (see (3.22)). We chose, therefore, to apply (without any real loss in generality) a Dirichlet boundary condition at the boundary $x = 0$ ($b(0, t) = \beta_0$, for all $t > 0$) for the numerical results described below. Figures 6a, 6b present the concentration profiles for a and b in the case $\phi = 1.0$, $\beta_0 = 1.0$. These show the propagation of travelling waves of permanent form which move with constant velocity. The numerical integrations give that the b travelling wave leaves behind a region where b is a constant b_s (with $b_s = 1.854$) and that this wave is moving with the minimum possible speed $v = v_{\min} = 2.172$ in this case. The value attained at the rear of the wave is independent of the concentration of the reservoir (being an intrinsic feature of the long time structure developed) as several numerical

integrations with different values of β_0 show in Figures 7a (with $\beta_0 = 0.5$) and 7b (with $\beta_0 = 2.0$). Finally, we checked the influence of varying the flow rate ϕ upon the movement of the reaction-diffusion-convection front. Figure 8 shows the result of the front position, x_w , as a function of time for three different flow rates ϕ (here $\phi = 0, 1.0$ and 5.0 respectively) showing that the long time evolving structure is travelling with a constant velocity given by the slopes of the straight lines appearing in the figure. These slopes correlate well with the values of the wave speed obtained from the numerical integrations of Equations (2.2, 2.3). As expected the larger the ϕ the faster the wave propagates.

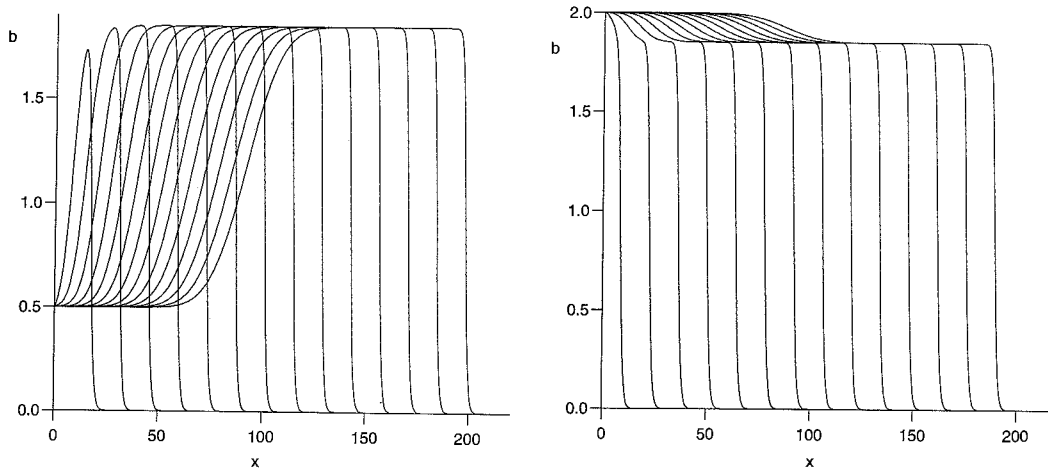


Figure 7. Concentration profiles for $\phi = 1.0$ and two different values of β_0 : (a) $\beta_0 = 0.5$, (b) $\beta_0 = 2.0$ (cubic autocatalysis).

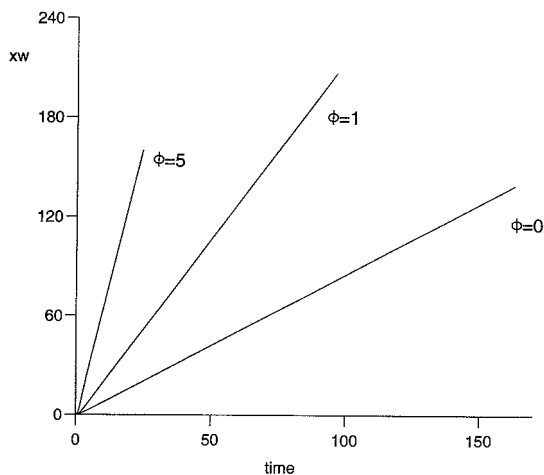


Figure 8. Successive positions of the TWS for $\beta_0 = 1.0$ and three different values of ϕ : $\phi = 0, 1, 5$ (cubic autocatalysis).

4. Conclusions

In this paper we studied a simple prototype model for a differential flow reactor which accounts for the effects of applying a flow of autocatalyst in a system with simple reaction kinetics. This problem falls into the larger context of studying the possible destabilisation of the homogeneous reference state of a chemical system which causes the medium to self-organise into a pattern of travelling waves through the differential flow instability, the so called DIFICI mechanism as mentioned in the Introduction. However, in all the previous work on the DIFICI context the theoretical framework was set up using a circular flow reactor (with corresponding periodic boundary conditions being applied at its ends). This is not very realistic and thus motivates our present work which considered a differential flow reactor in a form of a long, thin tube (with the transversal effects being neglected). A reaction is then initiated based on the autocatalytic kinetics $A + mB \rightarrow (m + 1)B$, rate kab^m ($m = 1, 2$). The physical problem considered is a practical experimental situation in which the reactant A (present initially at uniform concentration everywhere) is immobilised within the reactor. The differential flow mechanism manifests then via the flow (with constant velocity) and diffusion of the autocatalytic species through the reaction region.

We considered the spatio-temporal structures supported by such a physical configuration by analysing the resulting equations in some detail. Although no instabilities were found we showed that the system can support permanent form travelling-wave solutions (TWS), establishing the properties of these minimum speed TWS in terms of the parameters of the problem. Further insights into these solutions were provided by the analysis of the full initial-value problem (IVP) for which, in the main two cases of interest ($m = 1, 2$) we established that that these are the only long-time solutions supported. This follows from the properties of uniqueness and global existence for the solutions of the IVP derived in Section 3.2. The numerical solutions have confirmed the analytical results and have shown that in all the cases the long time solution evolved into a travelling reaction-diffusion wave with permanent form propagating with its minimum possible speed thus suggesting that these are stable. At the rear of this wave there is a region in which the concentration of reactant A is zero with that of B given by (2.7). Then there is an adjustment of this to the autocatalyst reservoir concentration through a convection-diffusion wave which propagates with speed $\phi < v_{\min}$; these two waves are consequently separating relative to each other.

We expect to encounter more interesting behaviour in a differential flow reactor with a similar physical configuration but with chemistry being based on a more realistic (and complicated) kinetics such as the cubic autocatalator (or the Gray–Scott model). This situation is presently being considered in detail by the authors.

Appendix

Here we establish the validity of the assertions (1) and (2) of Lemma 1.

Equation (3.11) is readily solved to get, on using the notation $c = b_0 > 0$

$$\frac{\ln B}{(1+c)^2} - \frac{\ln(1+c-B)}{(1+c)^2} - \frac{1}{B(1+c)} = \frac{\ln c}{(1+c)^2} - \frac{1}{c(1+c)} + t \quad \text{for all } t > 0. \quad (\text{A1})$$

From (A1) we then find, with the notation $B' = \partial B / \partial c$, that

$$c^2(1+c)B' = 2(cB)^2(1+c-B)t + B^2(1+c-B) + c^2B > 0 \quad \text{for all } t > 0, \quad (\text{A2})$$

since

$$c \leq B < 1 + c \quad \text{for all } t > 0. \quad (\text{A3})$$

This establishes the first assertion of the lemma. We then differentiate A2 once more with respect to c to get, after some calculation

$$cB'' = B^2 G(c, B, t), \quad (\text{A4})$$

where G is the polynomial

$$\begin{aligned} G(c, B, t) = & (1 + c - B)(8t^2 c^5 B + 6tc^4 + 8t^2 c^4 B \\ & - 12t^2 c^4 B^2 + 8tc^3 B + c^2 - 12t(cB)^2 + \\ & + 8tc^2 B - 2c + 2cB + 2B - 3B^3). \end{aligned} \quad (\text{A5})$$

This can also be written as

$$G(c, B, t) = (1 + c - B)(C_2(c, B)t^2 + C_1(C, B)t + C_0(c, B)), \quad (\text{A6})$$

with

$$C_2(c, B) = 4c^4 B(2 + 2c - 3B), \quad (\text{A7})$$

$$C_1(c, B) = 2c^2(-6B^2 + 4(1 + c)B + 3c^2), \quad (\text{A8})$$

$$C_0(c, B) = (c - B)(c - 2 + 3B). \quad (\text{A9})$$

From (A7–A9) it is readily established that

$$C_2 < 0 \quad \text{for all } c > 2, \quad C_1 > 0 \quad \text{and} \quad C_0 < 0 \quad \text{for all } c > 0. \quad (\text{A10})$$

From (A4, A6–A10) we then have that the sign of B'' is given by the sign of

$$4C_2 C_0 - C_1^2 = -4c^5(-2(1 + c)B^2 + 16(1 + c)^2 B + 9c^3), \quad (\text{A10})$$

which is found to be negative for all

$$c \geq c^* = 24.9738\dots \quad (\text{A11})$$

Thus we conclude that for all $c \geq c^*$ we have $B'' < 0$ for all $t > 0$ which establishes the second assertion and our lemma is proved.

Acknowledgements

We would like to thank Professor B.D. Sleeman (Leeds University) for suggesting the use of Weissler's idea for getting an upper solution for b in the case $m = 2$. RAS acknowledges the financial support from ORS and Leeds University.

References

1. R. Kapral and K. Showalter (eds), *Chemical Waves and Patterns*. Dordrecht: Kluwer Academic Publishers (1995) 640 pp.

2. M.A. Marek, S.C. Müller, T. Yamaguchi and K. Yoshikawa (eds), *Dynamism and Regulation in Nonlinear Chemical Systems*. Amsterdam: North-Holland (1995) 317 pp. See also the special issue of *Physica D* 84 (1995).
3. B.R. Johnson and S.K. Scott, New approaches to chemical patterns. *Chem. Soc. Rev.* 25 (1996) 265–273.
4. A.M. Turing, The chemical basis of morphogenesis. *Philos. Trans. Roy. Soc.* B327 (1952) 37–72.
5. J.D. Murray, *Mathematical Biology*. Berlin: Springer-Verlag (1990) 767 pp.
6. V. Castets, E. Dulos, J. Boissonade and P. DeKepper, Experimental evidence of a sustained standing Turing-type non-equilibrium chemical pattern. *Phys. Rev. Lett.* 64 (1990) 2953–2965.
7. I.R. Epstein and I. Lengyel, Turing structures. Progress toward a room temperature, closed system. *Physica D* 84 (1995) 1–11.
8. A.B. Rovinsky and M. Menzinger, Chemical instability induced by a differential flow. *Phys. Rev. Letters* 69 (1992) 1193–1196.
9. A.B. Rovinsky and M. Menzinger, Self-organisation induced by the differential flow of activator and inhibitor. *Phys. Rev. Letters* 70 (1993) 778–781.
10. M. Menzinger and A.B. Rovinsky, The differential flow instabilities. In: R. Kapral and K. Showalter (eds), *Chemical Waves and Patterns*. Dordrecht: Kluwer Academic Publishers (1995) 365–397.
11. X.-G. Wu, S. Nakata, M. Menzinger and A.B. Rovinsky, Differential flow instability in a tubular flow reactor: its convective nature. *J. Phys. Chem.* 100 (1996) 15810–15814.
12. S. Ponce Dawson, A. Lawniczak and R. Kapral, Interactions of Turing and flow-induced chemical instabilities. *J. Chem. Phys.* 100 (1994) 5211–5218.
13. R.A. Satnoianu, J.H. Merkin and S.K. Scott, Differential flow induced instability in a cubic autocatalator system. To appear in *J. Eng. Math.*
14. M.J. Metcalf, J.H. Merkin and S.K. Scott, Oscillating wave fronts in isothermal chemical systems with arbitrary powers of autocatalysis. *Proc. R. Soc. Lond. A* 447 (1994) 155–174.
15. A. Saul and K. Showalter, Propagation reaction-diffusion fronts. In: R.J. Field and M. Burger (eds), *Oscillations and Travelling Waves in Chemical Systems*. New York: Wiley (1985) 681 pp.
16. R.J. Field and R.M. Noyes, Oscillations in chemical systems. IV Limit cycle behaviour in a model of a real chemical reaction, *J. Chem. Soc.* 60 (1974) 1877–1884.
17. J.H. Merkin, D.J. Needham and S.K. Scott, A simple model for sustained oscillations in isothermal chain-branching or autocatalytic reactions in a well stirred, open system. *Proc. R. Soc. Lond. A* 398 (1985) 81–116.
18. E.E. Selkov, Self-oscillations in glycolysis, I. A simple kinetic model. *Eur. J. Biochem.* 4 (1968) 79–86.
19. J. Billingham and D.J. Needham, The development of travelling waves in quadratic and cubic autocatalysis with unequal diffusion rates. I. Permanent form travelling waves. *Phil. Trans. R. Soc. Lond. A* 334 (1991) 1–25.
20. J. Billingham and D.J. Needham, A note on the properties of a family of travelling-wave solutions arising in cubic autocatalysis. *Dynamics and Stability of Systems*, 6 (1991) 33–49.
21. J. Billingham and D.J. Needham, The development of travelling waves in quadratic and cubic autocatalysis with unequal diffusion rates. III: Large time development in quadratic autocatalysis. *Quart. Appl. Math.* L2 (1992) 343–372.
22. J.H. Merkin and D.J. Needham, Propagating reaction-diffusion waves in a simple isothermal quadratic autocatalytic chemical system. *J. Eng. Math.* 23 (1989) 343–356.
23. J.H. Merkin, D.J. Needham and S.K. Scott, The development of travelling waves in a simple isothermal chemical system. I. Quadratic autocatalysis with linear decay. *Proc. R. Soc. Lond. A* 424 (1989) 187–209.
24. D.J. Needham and J.H. Merkin, The development of travelling waves in a simple isothermal chemical system with general orders of autocatalysis and decay. *Proc. R. Soc. Lond. A* 337 (1991) 261–274.
25. J.H. Merkin and D.J. Needham, Reaction-diffusion waves in an isothermal chemical system with general orders of autocatalysis and spatial dimension. *ZAMP* 44 (1993) 707–721.
26. J. Guckenheimer and P. Holmes, *Nonlinear Oscillators, Dynamical Systems and Bifurcation of Vector Fields*. New York: Springer-Verlag, second printing (1986) 459 pp.
27. J.H. Merkin, D.J. Needham and S.K. Scott, Coupled reaction-diffusion waves in an isothermal autocatalytic chemical system. *IMA J. Appl. Math.* 50 (1993) 43–76.
28. J. Smoller, *Shock Waves and Reaction-Diffusion Equations*. New York: Springer-Verlag second edition (1994) 632 pp.
29. P. Grindrod, *Patterns and Waves (The Theory and Applications of Reaction-Diffusion Equations)*. Oxford: Clarendon Press (1991) 239 pp.
30. D. Henry, *Geometrical Theory of Semilinear Parabolic Equations*. New York: Springer-Verlag, Lectures Notes in Math. 840 (1981) 348 pp.
31. F.B. Weissler, Single point blow-up of semilinear initial value problem. *J. Diff. Eqs.* 55 (1984) 204–224.